A Semi-analytical Approach for Masonry Arch Dynamics

Anna Sinopoli

Abstract A semi-analytical approach is proposed for modelling the plane dynamics of a masonry arch, treated as a system of rigid elements with friction and unilateral contacts at each joint. By generalising the method proposed in previous research, the analytical approach is firstly applied to the plane dynamics of a rectangular block simply supported on a moving base. In this case, where the contact although sometimes extended is unique, dynamics is formulated as a frictional contact problem, and conditions for onset of motion according to various mechanisms are fully analytically identified; moreover, criteria for evaluating contact reactions during either smooth or non-smooth dynamics are outlined. The method is then extended to the case of the arch, where each element is characterized at most by a double extended contact; criteria for the onset of motion and evaluation for each element of contact reactions during the dynamic evolution are then identified. The approach proposed constitutes a first step for performing dynamic analysis through either an event-driven or a time-stepping numerical procedure.

Keywords Signorini-Coulomb law • Non-smooth contact dynamics • Masonry arch

1 Introduction

The development of the plastic theory in the 1950s and Heyman's basic idea of transferring its philosophy from the steel to stone skeleton (Heyman 1969) made it possible to state the limit analysis of masonry arches for standard behaviour as a linear complementarity problem (Gilbert and Melbourne 1994); in this case, bounding theorems allow for determining collapse from either below or from above without distinction. In the presence of finite friction, on the contrary, the normality rule does not hold and non-associated flow rule invalidates bounding theorems; modified criteria must then be defined, on the basis of which computational strategies can be

A. Sinopoli (✉)
Department of Structural and Geotechnical Engineering, Sapienza University , Via Occorsio 8, 30039 Stra, Venezia, Italy
e-mail: anna.sinopoli@uniroma1.it

D. Aita et al. (eds.), *Masonry Structures: Between Mechanics and Architecture*,
DOI 10.1007/978-3-319-13003-3_5

adopted (Livesley 1978; Sinopoli et al. 1997; Baggio and Trovalusci 2000; Orduna and Lourenço 2005). The problem is generally formulated by using non-linear programming, and searching for the optimal solution is difficult not only because of numerical calculations; the absence of stability criteria makes it possible to find an optimal solution which is not a global minimum.

Recently, a simple method has been proposed (Sinopoli et al. 2007), in the framework of contact mechanics, for the collapse analysis with finite friction of a semicircular arch under its own weight. In this respect, it is worthwhile observing that, if the collapse condition is considered as that separating equilibrium from starting motion, the best framework for identifying it is in dynamics; the collapse condition thus transforms into the starting mechanism of the motion. Moreover, dynamics formulated as a contact problem, through the decomposition in sub-problems for which appropriate flow rules can be defined, eliminates the typical indeterminacy of any static approach.

While numerous papers have been produced on limit analysis, it is surprising that masonry arch dynamics is a subject to which little attention has been paid in the literature, despite the fact that the preservation of the monumental patrimony against seismic risk has promoted research during the last decades on stone or masonry structures, modelled as assemblage of blocks with frictional contacts. Starting with Housner's model (Housner 1963), the main aspects of dynamics became a new field of research: classical questions of Coulomb friction (Lötstedt 1982); structural behaviour (Spanos and Koh 1984; Sinopoli 1987); stability of the responses and transition to chaos (Hogan 1990; Ageno and Sinopoli 2005, 2010); impact and dynamic modelling (Sinopoli 1987, 1997; Moreau 1988, 1999, 2005; Augusti and Sinopoli 1992); and, finally, numerical codes (Glocker and Pfeiffer 1992; Jean 1999).

Oppenheim (1992) was the first to propose a semi-analytical model to investigate the dynamics of an arch, treated as a four-link mechanism—that is, a single degree of freedom system—subjected to a base impulse acceleration; the dynamics equation was obtained by a classical Lagrangian formulation and numerically integrated. The same model was adopted in later papers (Clemente 1998; De Lorenzis et al. 2007). De Lorenzis et al. (2007) also made a comparison with results obtained using the commercial program UDEC (Cundall and Strack 1979). More recently, a stone arched structure has been investigated (Rafiee et al. 2008) with a discrete elements method using the platform LMGC90, based on the non-smooth contact dynamics method (Jean 1999).

It is obvious that difficulties inherent in analytical modelling encourage the use of numerical methods. Nevertheless, although mechanical modelling of un-reinforced masonry remains a challenging problem, the focusing of numerical methods has mainly been concentrated in discussing computational algorithms.

In this present paper I extend my previous research on the dynamics of a rigid body simply supported on a moving boundary (Sinopoli 1997). The new approach for the dynamics, formulated as a contact problem governed by Signorini's and Coulomb's laws (Sinopoli 2010), is oriented to the dynamical modelling of the masonry arch treated as a system of n rigid voussoirs, with frictional and unilateral

contacts at each joint. First, the modelling is given for the single block, to guide the understanding on how contact laws can be checked, by identifying at the contact point both the value of the generalised reaction and persistency or variation of the activated mechanism; we refer to the relationships between initial conditions, active forces and contact reactions. The formulation is then extended to the arch; new questions related to its typology—indeterminacy due to double contacts and elements number—are then discussed and solved. The formulation allows the implementation of a numerical platform, based on either implicit time-stepping or explicit event-driven numerical method for integrating the equations of motion; the platform, outside the scope of the present paper due to its complexity, is a target of future research.

2 Single Block Dynamics

Consider a rectangular rigid block free-standing with Coulomb friction on rigid ground Γ, which moves by a translational horizontal motion $\ddot{x}_O = k_s(t)g$, where g is the gravity acceleration. Refer the dynamics to the system (O, x, y) fixed on Γ, with which unit vectors $(\boldsymbol{t}, \boldsymbol{n})$ are associated; $\boldsymbol{n}$ is outwards oriented (For the definition of the symbols used in what follows, see the Appendix "List of Symbols").

2.1 Kinematics

Assume the position of the mass centre G and rotation angle to be Lagrangian coordinates; thus, the motion of the body transforms into the path of its representative point in the configuration space, where the kinetic energy metrics is assumed in order to preserve the Euclidean structure (Moreau 1988; Sinopoli 1997). Through the linear mapping induced by Lagrangian coordinates, the velocity of any point P of the body becomes:

$$\dot{\boldsymbol{r}}_{\mathrm{P}} = \mathbf{N}_{\mathrm{P}}^{\mathrm{T}}\, \dot{\boldsymbol{u}} \tag{1}$$

where $\mathbf{N}_{\mathrm{P}}^{\mathrm{T}}$ is the $[2 \times 3]$ gradient operator of the mapping, $\dot{\boldsymbol{u}}$ the generalised velocity and apex T indicates transposition. According to (1), tangential and normal components of $\dot{r}_P$ are:

$$\begin{aligned} \dot{r}_{\mathrm{P,t}} &= \boldsymbol{N}_{\mathrm{P,t}}{}^{T} \dot{\boldsymbol{u}} \\ \dot{r}_{\mathrm{P,n}} &= \boldsymbol{N}_{\mathrm{P,n}}{}^{T} \dot{\boldsymbol{u}} \end{aligned} \tag{2}$$

Note that $\boldsymbol{N}_{\mathrm{P,t}}$ and $\boldsymbol{N}_{\mathrm{P,n}}$ are generalised directions starting at P and associated with $\boldsymbol{t}$ and $\boldsymbol{n}$, respectively (Fig. 1).

If the body, initially at rest, is in contact with the ground along the side AB, the boundary impenetrability allows only positive or null values of the normal

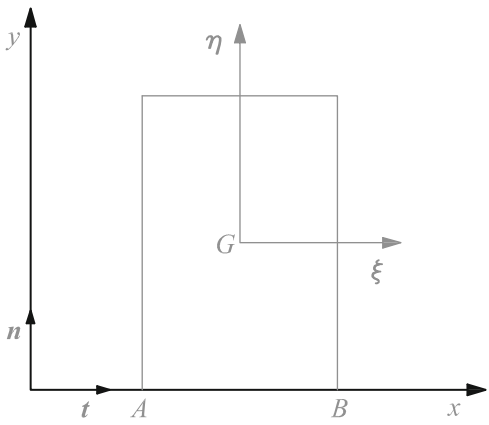

Fig. 1 The rigid block

virtual displacement of contact points. Since virtual displacements and velocities have the same structure, the impenetrability transforms into a unilateral constraint to be satisfied by admissible velocities $\dot{\boldsymbol{u}}$ of the body:

$$\overline{\dot{r}_{\mathrm{P,n}}} = \boldsymbol{N}_{\mathrm{P,n}}^{\mathrm{T}} \dot{\boldsymbol{u}} \geq 0 \quad \forall P \in AB \tag{3}$$

The set (3) contains the velocity at instant t, if it exists; on the contrary, it must be interpreted as the right-sided velocities set if velocity does not exist, as is the case of an impact occurring when either one or multiple points enter into contact coming from a no-contact situation.

2.2 Normal and Tangential Contact Laws

Normal contact (3) is guaranteed by reaction $R_{\mathrm{n}} \geq 0$, acting at the unknown contact centre Q. According to mapping, forces are transformed through the invariance of the work, so that normal and tangential generalised reactions become:

$$\begin{aligned} \boldsymbol{\Psi}_{\mathrm{Q,t}} &= R_{\mathrm{t}} \, \boldsymbol{N}_{\mathrm{Q,t}} \\ \boldsymbol{\Psi}_{\mathrm{Q,n}} &= R_{\mathrm{n}} \, \boldsymbol{N}_{\mathrm{Q,n}} \end{aligned} \tag{4}$$

At any time t, contact is lost if $\dot{r}_{\mathrm{Q,n}} > 0$, so that $R_{\mathrm{n}} = 0$; while contact is maintained if $\dot{r}_{\mathrm{Q,n}} = 0$, with $R_{\mathrm{n}} \geq 0$. The law of normal contact is thus the well-known Signorini's law (Fig. 2):

$$\begin{aligned} &\dot{r}_{\mathrm{Q,n}} \geq 0 \\ &R_{\mathrm{n}} \geq 0 \\ &\boldsymbol{\Psi}_{\mathrm{Q,n}}^{\mathrm{T}} \dot{\boldsymbol{u}} = 0 \end{aligned} \tag{5}$$

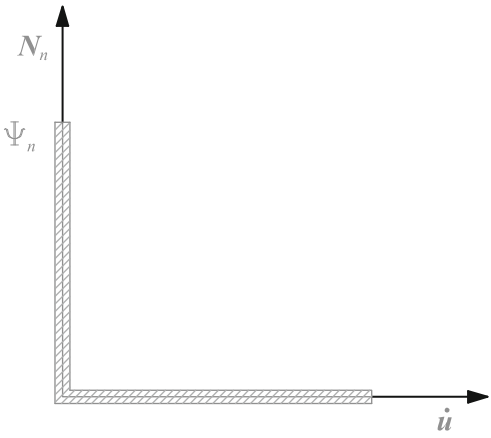

Fig. 2 Signorini's law

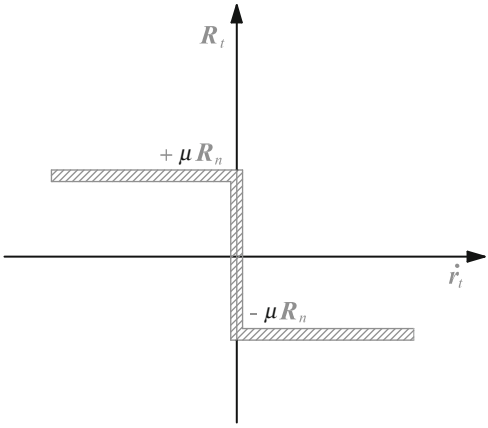

Fig. 3 Coulomb's law

Note that vector $\boldsymbol{N}_{\mathrm{Q,n}}$ is orthogonal to $\dot{\boldsymbol{u}}$, while values of R_{n} determines a positive flux along $\boldsymbol{N}_{\mathrm{Q,n}}$ giving $\boldsymbol{\Psi}_{\mathrm{Q,n}}$.

The tangential contact is governed by Coulomb's law (Fig. 3):

$$\begin{aligned} &R_{\mathrm{t}} = -\mu\, sgn(\dot{r}_{\mathrm{Q,t}})R_{\mathrm{n}} && \text{for } :\dot{r}_{\mathrm{Q,t}} \neq 0 \\ &\left|R_{\mathrm{t}}\right| \leq \mu\, R_{\mathrm{n}} && \text{for } :\dot{r}_{\mathrm{Q,t}} = 0 \\ &\boldsymbol{\Psi}_{\mathrm{Q,t}}{}^{\mathrm{T}}\dot{\boldsymbol{u}} \leq \boldsymbol{0} \end{aligned} \tag{6}$$

corresponding to maximal dissipation if $\boldsymbol{\Psi}^{*}_{\mathrm{Q,t}}$ is a generic solution belonging to Coulomb's cone:

$$\left(\boldsymbol{\Psi}^{*}_{\mathrm{Q,t}} - \boldsymbol{\Psi}_{\mathrm{Q,t}}\right)^{\mathrm{T}}\dot{\boldsymbol{u}} \geq \boldsymbol{0} \tag{7}$$

Normal and tangential contact laws also hold during an impact, where reactions are associated with Dirac's distributions. By assuming inelastic impact, that is when the impact ends as soon as the normal velocity of Q becomes zero, contact laws in terms of right-sided velocities (apex $+$) are, respectively:

$$\begin{aligned} &\dot{r}^{+}_{\mathrm{Q,n}} = 0 \\ &I_{\mathrm{n}} \geq 0 \\ &\Xi^{\mathrm{T}}_{\mathrm{Q,n}} \dot{\boldsymbol{u}}^{+} = 0 \end{aligned} \tag{8}$$

and:

$$\begin{aligned} &I_{\mathrm{t}} = -\boldsymbol{\mu}\ sgn\left(\dot{r}^{+}_{\mathrm{Q,t}}\right) I_{\mathrm{n}} \qquad &&\text{for}: \ \dot{r}^{+}_{\mathrm{Q,t}} \neq 0 \\ &|I_{\mathrm{t}}| \leq \boldsymbol{\mu}\ I_{\mathrm{n}} \qquad &&\text{for}: \ \dot{r}^{+}_{\mathrm{Q,t}} = 0 \\ &\Xi^{\mathrm{T}}_{\mathrm{Q,t}} \dot{\boldsymbol{u}}^{+} \leq 0 \end{aligned} \tag{9}$$

The unilateral frictional contact results thus into two sub-problems which are connected to each other since tangential reaction depends on the normal one, and reciprocally. Dynamics with friction and unilateral contact can therefore be tackled by solving in turns the two sub-problems until convergence.

2.3 Dynamics Equation

Derive the equation of dynamics from d'Alembert's principle; in terms of generalised forces—active $\boldsymbol{S}$ and reactive $\boldsymbol{\Psi}_{\mathrm{Q}}$—and virtual velocity $\bar{\dot{\boldsymbol{u}}}$ it is:

$$\ddot{\boldsymbol{u}}^{\mathrm{T}} \bar{\dot{\boldsymbol{u}}} = \left(\boldsymbol{S} + \boldsymbol{\Psi}_{\mathrm{Q,t}} + \boldsymbol{\Psi}_{\mathrm{Q,n}}\right)^{\mathrm{T}} \bar{\dot{\boldsymbol{u}}} \tag{10}$$

Since the contact laws do not reduce the degrees of freedom, the equation of motion can have a time-variant structure; thus, the transition from one mechanism to another consistent with contact laws induces a strongly non-linear character of dynamics, which can also exhibit phases of impulsive motion. In this last case, the dynamics equation (10) becomes:

$$\Delta\dot{\boldsymbol{u}}^{\mathrm{T}} \bar{\dot{\boldsymbol{u}}}^{+} = \left(\Xi_{\mathrm{Q,t}} + \Xi_{\mathrm{Q,n}}\right)^{\mathrm{T}} \bar{\dot{\boldsymbol{u}}}^{+} \tag{11}$$

A unilateral frictional contact introduces two kinds of difficulties: firstly, contact reactions are unknown; secondly, when the system is at rest or after an impact, the starting mechanism is also unknown. The starting mechanism is extremely important for practical purposes, as is the protection of art objects or technical instruments, which can be damaged during earthquakes. Knowing how the starting mechanism depends on the excitation and system features could provide useful indications for passive protection devices.

2.4 Starting Motion and Dynamic Balance

With reference to Eq. (10), observe that reactive forces are requested to modulate dynamics in accordance with contact laws; so, their virtual power cannot be positive. The necessary condition for starting motion is therefore that in correspondence to an admissible mechanism $\bar{\dot{\boldsymbol{u}}}$:

$$\boldsymbol{S}^{\mathrm{T}}\bar{\dot{\boldsymbol{u}}} \geq 0 \tag{12}$$

For conservative active forces and friction large enough, inequality (12) satisfied as equality corresponds to a stability criterion; thus, if satisfied for the lowest value of $\boldsymbol{S}$:

$$\min_{\boldsymbol{S}} \left(\boldsymbol{S}^{\mathrm{T}}\bar{\dot{\boldsymbol{u}}} \right) = 0 \tag{13}$$

it gives the closest unstable equilibrium configuration. For finite friction, on the contrary, relationship (13) must be interpreted as a necessary but not sufficient condition; among admissible mechanisms $\bar{\dot{\boldsymbol{u}}}$ it selects the candidates with no sliding at the contact point. The activation of the actual mechanism—the sufficient condition—requires that contact laws be satisfied. For example, in the case of the block of Fig. 1 subjected to its own weight and excited by a horizontal ground motion $\ddot{x}_{\mathrm{O}} = k_{\mathrm{s}}(0)g$ with $k_{\mathrm{s}}(0) > 0$, in accordance with inequality (3), admissible mechanisms maintaining normal contact without sliding are: the null mechanism $\dot{\boldsymbol{u}} = \boldsymbol{0}$, corresponding to resting and contact at any point of AB, and the rocking mechanism $\dot{\boldsymbol{u}}_{\mathrm{A}} \neq \boldsymbol{0}$ with contact at point A. This means that identification of the starting mechanism coincides with that of unknown contact centre Q; therefore, consider mechanism $\dot{\boldsymbol{u}}_{\mathrm{Q}}$ with the centre of instantaneous rotation at Q, and express the tangential position of Q as a linear combination of A and B positions:

$$r_{\mathrm{Q,t}} = (1 - e)\, r_{\mathrm{A,t}} + e\, r_{\mathrm{B,t}} \qquad 0 \leq e \leq 1 \tag{14}$$

Mechanism $\dot{\boldsymbol{u}}_{\mathrm{Q}}$ in Eq. (13) allows for identifying the value of e and contact centre Q, that is, the mechanism as a function of $k_{\mathrm{s}}(0)$. If b and h are the base and height lengths, respectively, and friction is large enough, for $k_{\mathrm{s}}(0) < b/h$ the contact centre Q is internal to AB, with $\dot{\boldsymbol{u}}_{\mathrm{Q}} = \boldsymbol{0}$, so that the block remains at rest; while the contact centre is at point A, corresponding to both resting $\dot{\boldsymbol{u}} = \boldsymbol{0}$ and rocking mechanism $\dot{\boldsymbol{u}}_{\mathrm{A}}$ for $k_{\mathrm{s}}(0) = b/h$, so that the equilibrium configuration becomes unstable and rocking can start for $k_{\mathrm{s}}(0) \geq b/h$.

If the sticking assumption is removed, admissible sliding-rocking mechanisms $\bar{\dot{\boldsymbol{u}}} \neq \boldsymbol{0}$ exist with normal contact maintained at A. Thus, Eq. (13) gives, for any force centre internal to AB, that is for $k_{\mathrm{s}}(0) < b/h$, sliding-rocking mechanisms corresponding to indifferent equilibrium condition, that is to resting; the unique sliding-rocking mechanism corresponding to unstable equilibrium configuration is

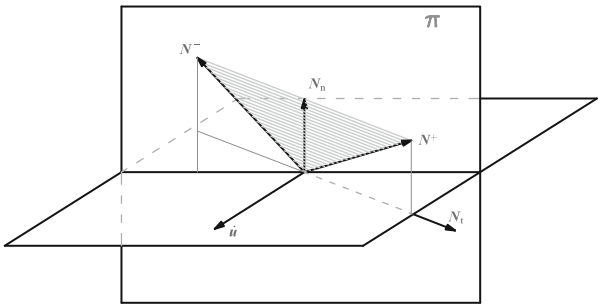

Fig. 4 Vectors $\boldsymbol{N}_{\mathrm{A,t}}$ and $\boldsymbol{N}_{\mathrm{A,n}}$ and Coulomb cone, in plane π

$\dot{\boldsymbol{u}}_{\mathrm{A}}$, for $k_{\mathrm{s}}(0) = b/h$, so that necessary conditions to activate sliding-rocking and rocking coincide with contact at point A and $k_{\mathrm{s}}(0) \geq b/h$.

To identify the sufficient condition, perform the dynamic balance of equation (10) for rocking with contact at point A:

$$\ddot{\boldsymbol{u}}_{\mathrm{A}} = \boldsymbol{S} + \boldsymbol{\Psi}_{\mathrm{A,t}} + \boldsymbol{\Psi}_{\mathrm{A,n}} \tag{15}$$

The analysis here proposed, although aimed at identifying the starting motion, holds also at any time of dynamics according to a given mechanism, if the tangential velocity of the contact point is zero. Assume $k_{\mathrm{s}}(0) \geq b/h$, and observe that, if both tangent and normal contact have to be maintained, from relationships:

$$\begin{aligned} \dot{r}_{\mathrm{A,t}} &= \boldsymbol{N}_{\mathrm{A,t}}{}^{\mathrm{T}}\dot{\boldsymbol{u}}_{\mathrm{A}} = 0 \\ \dot{r}_{\mathrm{A,n}} &= \boldsymbol{N}_{\mathrm{A,n}}{}^{\mathrm{T}}\dot{\boldsymbol{u}}_{\mathrm{A}} = 0 \end{aligned} \tag{16}$$

it follows that both vectors $\boldsymbol{N}_{\mathrm{A,t}}$ and $\boldsymbol{N}_{\mathrm{A,n}}$ lie on the plane π orthogonal to the mechanism $\dot{\boldsymbol{u}}_{\mathrm{A}}$ (Fig. 4).

Moreover, both acceleration components of point A consists of two terms:

$$\begin{aligned} \ddot{r}_{\mathrm{A,t}} &= \boldsymbol{N}_{\mathrm{A,t}}{}^{\mathrm{T}}\ddot{\boldsymbol{u}}_{\mathrm{A}} + \dot{\boldsymbol{N}}_{\mathrm{A,t}}{}^{\mathrm{T}}\dot{\boldsymbol{u}}_{\mathrm{A}} = 0 \\ \ddot{r}_{\mathrm{A,n}} &= \boldsymbol{N}_{\mathrm{A,n}}{}^{\mathrm{T}}\ddot{\boldsymbol{u}}_{\mathrm{A}} + \dot{\boldsymbol{N}}_{\mathrm{A,n}}{}^{\mathrm{T}}\dot{\boldsymbol{u}}_{\mathrm{A}} = 0 \end{aligned} \tag{17}$$

the first parallel to the corresponding component of $\ddot{r}_A$ and the second—the centripetal acceleration—depending on initial conditions and oriented from A to G. For the reciprocity between points A and G considered as rotating each with respect to the other, it follows that acceleration $\ddot{\boldsymbol{u}}_{\mathrm{A}}$ is composed of two terms, the first parallel to $\dot{\boldsymbol{u}}_{\mathrm{A}}$ and the second lying on plane π with components:

$$\begin{aligned} \ddot{\boldsymbol{u}}_{\mathrm{A,t}} &= -\dot{\boldsymbol{N}}_{\mathrm{A,t}}{}^{\mathrm{T}}\dot{\boldsymbol{u}}_{\mathrm{A}} \\ \ddot{\boldsymbol{u}}_{\mathrm{A,n}} &= -\dot{\boldsymbol{N}}_{\mathrm{A,n}}{}^{\mathrm{T}}\dot{\boldsymbol{u}}_{\mathrm{A}} \end{aligned} \tag{18}$$

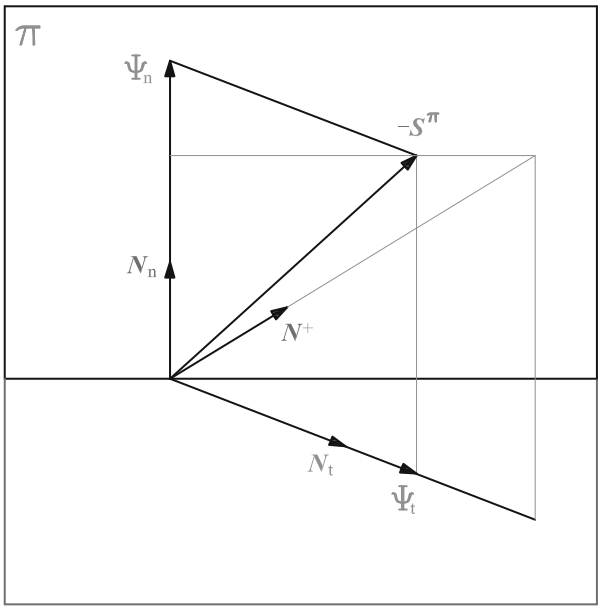

Fig. 5 Dynamic balance in the plane π

both strictly negative and oppositely directed with respect to $\ddot{N}_{A,t}$ and $\ddot{N}_{A,n}$, respectively.

By projecting Eq. (15) on plane π, that is, ignoring active force and acceleration components parallel to $\dot{\boldsymbol{u}}_{\mathrm{A}}$, which are allowed for maintaining contact, the dynamic balance becomes:

$$\ddot{\boldsymbol{u}}_{\mathrm{A,t}} + \ddot{\boldsymbol{u}}_{\mathrm{A,n}} - \boldsymbol{S}^{\pi} = \boldsymbol{\Psi}_{\mathrm{A,t}} + \boldsymbol{\Psi}_{\mathrm{A,n}} \tag{19}$$

where $\ddot{\boldsymbol{u}}_{\mathrm{A,t}}$ and $\ddot{\boldsymbol{u}}_{\mathrm{A,n}}$—the centripetal acceleration components—are known quantities and $\boldsymbol{\Psi}_{\mathrm{A,t}} = R_{\mathrm{t}}\boldsymbol{N}_{\mathrm{A,t}}$ and $\boldsymbol{\Psi}_{\mathrm{A,n}} = R_{\mathrm{n}}\boldsymbol{N}_{\mathrm{A,n}}$ are the unknowns to be determined according to Signorini's and Coulomb's laws. As shown in Figs. 4 and 5 (without subscript indicating contact point), vectors $\boldsymbol{N}_{\mathrm{A,t}}$ and $\boldsymbol{N}_{\mathrm{A,n}}$ identified in plane π Coulomb's cone through its boundaries:

$$\begin{aligned} \boldsymbol{N}_{\mathrm{A}}{}^{+} &= \boldsymbol{N}_{\mathrm{A,n}} + \mu\boldsymbol{N}_{\mathrm{A,t}} \\ \boldsymbol{N}_{\mathrm{A}}{}^{-} &= \boldsymbol{N}_{\mathrm{A,n}} - \mu\boldsymbol{N}_{\mathrm{A,t}} \end{aligned} \tag{20}$$

which are symmetric with respect to $\boldsymbol{N}_{\mathrm{A,n}}$ along the conjugate direction $\boldsymbol{N}_{\mathrm{A,t}}$.

Since centripetal terms are known, the dynamic balance is of a merely static nature. In particular, if the system is initially at rest, with null centripetal accelerations, and $-\boldsymbol{S}^{\pi}$ is internal to Coulomb's cone, generalised reactions are obtained by decomposing $-\boldsymbol{S}^{\pi}$ along $\boldsymbol{N}_{\mathrm{A,t}}$ and $\boldsymbol{N}_{\mathrm{A,n}}$ (Fig. 5).

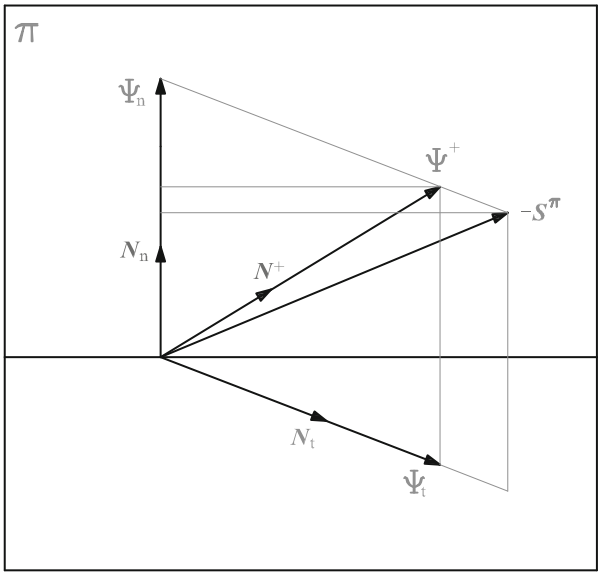

Fig. 6 Unbalance between active force and generalised reaction, for sliding-rocking

Note that since $\boldsymbol{N}_{\mathrm{A,t}}$ and $\boldsymbol{N}_{\mathrm{A,n}}$ are not orthogonal, the projection of $\boldsymbol{\Psi}_{\mathrm{A,t}}$ along $\boldsymbol{N}_{\mathrm{A,n}}$ gives the variation of $\boldsymbol{\Psi}_{\mathrm{A,n}}$ due to friction; this is the interplay between tangent and normal reactions of a frictional contact.

If the contact tangential velocity is zero, the sufficient condition for activating rocking is that: $\boldsymbol{\Psi}_{\mathrm{A,t}} \leq \mu R_{\mathrm{n}} \boldsymbol{N}_{\mathrm{A,t}}$, otherwise tangential contact cannot be maintained and tangential reaction is along the boundary of Coulomb's cone; both tangential and normal reactions are varied with respect to rocking, and the unbalanced component of $\boldsymbol{S}_{\pi}$ determines an acceleration opposite to $\boldsymbol{N}_{\mathrm{A,t}}$ (Fig. 6).

Similarly, for $k_s(0) < b/h$ the possibility of resting or the activation of sliding can be checked. The regions where each mechanism of the block, initially at rest, is activated are reported in Sinopoli (1997).

In conclusion, having satisfied the necessary condition to activate rocking and sliding-rocking, friction alone decides the activated mechanism. Thus, it is nonsense to say that sliding-rocking requires different values of $k_{\mathrm{s}}(0)$ with respect to rocking, since the energy dissipated by friction is balanced by the acceleration variation along $\boldsymbol{N}_{\mathrm{A,n}}$.

2.5 Dynamic Evolution for Smooth and Non-smooth Dynamics

During the motion, until both tangential and normal contact are maintained, the dynamic balance is in plane π, where Eq. (19) holds; in this case, vector $\dot{\boldsymbol{u}}_{\mathrm{A}}$ lies on

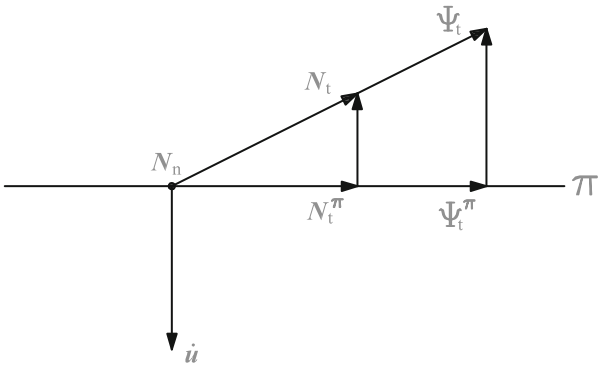

Fig. 7 Decomposition of tangential reaction, for sliding-rocking

the plane orthogonal to $\boldsymbol{N}_{\mathrm{A,n}}$, while $\boldsymbol{N}_{\mathrm{A,t}}$ and $\boldsymbol{N}_{\mathrm{A,n}}$ belong to the plane π orthogonal to $\dot{\boldsymbol{u}}_{\mathrm{A}}$ (Fig. 4). For lost tangential contact, that is, for $\ddot{r}_{A,t}$ —projection of $\ddot{\boldsymbol{u}}_{\mathrm{A}}$ along $\boldsymbol{N}_{\mathrm{A,t}}$—different from zero, $\boldsymbol{N}_{\mathrm{A,n}}$ is still orthogonal to $\dot{\boldsymbol{u}}_{\mathrm{A}}$, but vectors $\boldsymbol{N}_{\mathrm{A,t}}$ and $\boldsymbol{N}_{\mathrm{A,n}}$ lie on a plane π^* which is not orthogonal to $\dot{\boldsymbol{u}}_{\mathrm{A}}$. Nevertheless, since the contact balance is always on the positive hemi-space associated with $\boldsymbol{N}_{\mathrm{A,n}}$, the friction reaction $\boldsymbol{\Psi}_{\mathrm{A,t}} = R_{\mathrm{t}}\boldsymbol{N}_{\mathrm{A,t}}$ can be evaluated by decomposing it into two components (Fig. 7): the first parallel to $\dot{\boldsymbol{u}}_{\mathrm{A}}$, which determines a reduction of the velocity, and the second lying on plane π orthogonal to $\dot{\boldsymbol{u}}_{\mathrm{A}}$; both components depend on R_{t} through the corresponding decomposition of $\boldsymbol{N}_{\mathrm{A,t}}$. Thus, the problem can be solved on plane π by determining first R_{t} and then the resultant $\boldsymbol{\Psi}_{\mathrm{A,t}}$ along $\boldsymbol{N}_{\mathrm{A,t}}$.

In the case of an impact, the main problem is the identification of the post-impact mechanism. In accordance with contact laws (8) and (9), the dynamic balance (11) is:

$$\dot{\boldsymbol{u}}^{+\mathrm{T}}\overline{\dot{\boldsymbol{u}}^{+}} = \left(\dot{\boldsymbol{u}}^{-} + \Xi_{\mathrm{Q,t}} + \Xi_{\mathrm{Q,n}}\right)^{\mathrm{T}}\overline{\dot{\boldsymbol{u}}^{+}} \tag{21}$$

By comparing Eqs. (21) and (10), it follows that during an impact the role of the acceleration of smooth dynamics is played by the post-impact velocity, and that of the active force by pre-impact velocity. The procedure will therefore be the same followed for the starting mechanism of smooth dynamics, by treating pre-impact velocity $\dot{\boldsymbol{u}}^{-}$ as "active force", which makes it possible to determine both the velocity of post-impact motion and generalised impulses.

3 Arch Dynamics as an Assemblage of Discrete Elements

Consider an arch made of n rigid voussoirs, free standing with Coulomb friction on rigid ground Γ, which moves with a translational horizontal motion. Refer the dynamics of each voussoir to the system (O, x, y) fixed on Γ, with which unit vectors $(\boldsymbol{t}_0, \boldsymbol{n}_0)$ are associated; $\boldsymbol{n}_0$ is outwards oriented (Fig. 8).

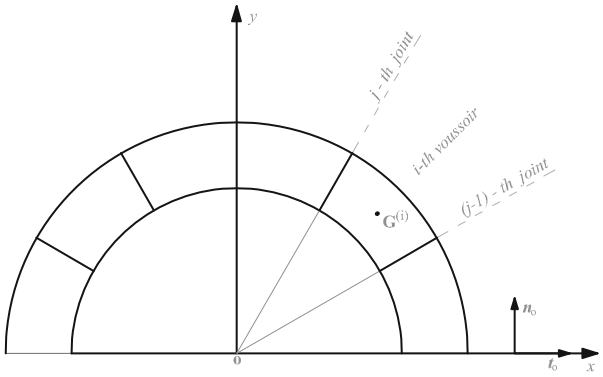

Fig. 8 Scheme of the arch as an assemblage of rigid voussoirs

Denote by i the counter of voussoirs, and number them from 1 to n; similarly, denote by j the counter of joints, and number them from 0 to n. When the arch is at rest, *j-th* joint is unique. During the motion, on the contrary, *j-th* joint can open and be split into two, the $j^{(\mathrm{i})}$-*th* and $j^{(\mathrm{i}+1)}$-*th* joints, bounding *i-th* and $(i+1)$-*th* voussoirs, respectively.

3.1 Kinematics and Contact Laws

Assume for generic *i-th* voussoir the position of the mass centre $G^{(\mathrm{i})}$ and rotation angle as Lagrangian coordinates, evaluated with respect to the system (O, x, y) fixed on Γ, and assume the kinetic energy metrics. If the arch is initially at rest, each voussoir is in full contact with two adjacent ones. In particular, at *j-th* joint, contact is maintained at point $Q^{(\mathrm{i}+1)}$, belonging to the lower boundary of $(i+1)$-*th* voussoir, and at point $P^{(\mathrm{i})}$ belonging to the upper boundary of *i-th* voussoir; denote points $Q^{(\mathrm{i}+1)}$ and $P^{(\mathrm{i})}$ as candidate and antagonist contact points at *j-th* joint. Thus, the couples of points maintaining contact for the *i-th* voussoir are $(Q^{(\mathrm{i}+1)}, P^{(\mathrm{i})})$ at the *j-th* joint, and $(Q^{(\mathrm{i})}, P^{(\mathrm{i}-1)})$ at $(j-1)$-*th* joint (Fig. 9). Through the mapping, velocities of points $Q^{(\mathrm{i}+1)}$ and $P^{(\mathrm{i})}$ become:

$$\begin{aligned} \dot{\boldsymbol{r}}_{\mathrm{Q}}^{(\mathrm{i}+1)} &= \mathbf{N}_{\mathrm{Q}}^{(\mathrm{i}+1)}\, \dot{\boldsymbol{u}}^{(\mathrm{i}+1)} \\ \dot{\boldsymbol{r}}_{\mathrm{P}}^{(\mathrm{i})} &= \mathbf{N}_{\mathrm{P}}^{(\mathrm{i})}\, \dot{\boldsymbol{u}}^{(\mathrm{i})} \end{aligned} \tag{22}$$

with analogous expressions for points $(Q^{(\mathrm{i})}, P^{(\mathrm{i}-1)})$ at $(j-1)$-*th* joint.

The impenetrability condition in this case bounds the normal velocity of the candidate point with respect to that of antagonist one, both evaluated on the local reference system fixed on the antagonist, and reciprocally; the unilateral constraint at each joint thus splits into two conditions. As an example, the impenetrability

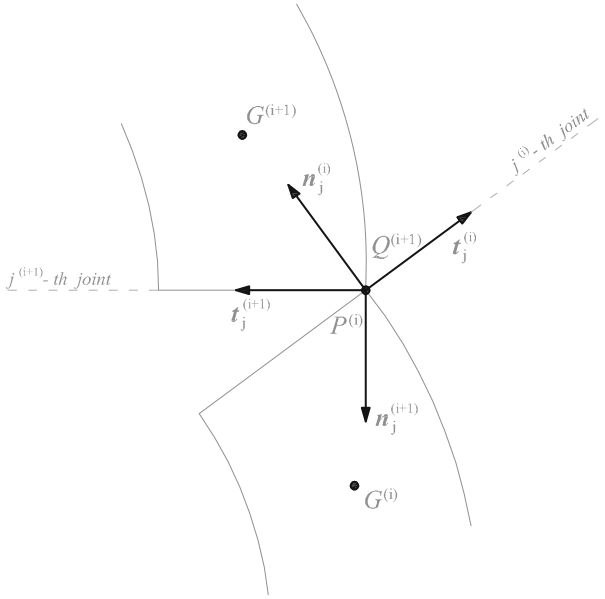

Fig. 9 Scheme of the contact, between *i-th* and $(i+1)$*-th* voussoirs

condition at *j-th* joint requires admissible velocities, evaluated in the local unit vectors system $(\boldsymbol{t}_j^{(i)}, \boldsymbol{n}_j^{(i)})$, fixed on $P^{(i)}$:

$$\begin{aligned}\dot{r}^{(i+1)}_{Q,n_j^{(i)}} - \dot{r}^{(i)}_{P,n_j^{(i)}} &= \boldsymbol{n}_j^{(i)^T}\left(\dot{\boldsymbol{r}}_Q^{(i+1)} - \dot{\boldsymbol{r}}_P^{(i)}\right) = \boldsymbol{n}_j^{(i)^T}\left(\mathbf{N}_Q^{(i+1)^T}\dot{\boldsymbol{u}}^{(i+1)} - \mathbf{N}_P^{(i)^T}\dot{\boldsymbol{u}}^{(i)}\right) = \\ &= \boldsymbol{H}^{(i+1)^T}_{Q,n_j^{(i)}}\dot{\boldsymbol{u}}^{(i+1)} - \boldsymbol{H}^{(i)^T}_{P,n_j^{(i)}}\dot{\boldsymbol{u}}^{(i)} \geq 0\end{aligned} \tag{23a}$$

and, reciprocally, in the local system $\left(\boldsymbol{t}_j^{(i+1)}, \boldsymbol{n}_j^{(i+1)}\right)$:

$$\begin{aligned}\dot{r}^{(i)}_{P,n_j^{(i+1)}} - \dot{r}^{(i+1)}_{Q,n_j^{(i+1)}} &= \boldsymbol{n}_j^{(i+1)^T}\left(\dot{\boldsymbol{r}}_P^{(i)} - \dot{\boldsymbol{r}}_Q^{(i+1)}\right) = \boldsymbol{n}_j^{(i+1)^T}\left(\mathbf{N}_P^{(i)^T}\dot{\boldsymbol{u}}^{(i)} - \mathbf{N}_{Q,n}^{(i+1)^T}\dot{\boldsymbol{u}}^{(i+1)}\right) = \\ &= \boldsymbol{H}^{(i)^T}_{P,n_j^{(i+1)}}\dot{\boldsymbol{u}}^{(i)} - \boldsymbol{H}^{(i+1)^T}_{Q,n_j^{(i+1)}}\dot{\boldsymbol{u}}^{(i+1)} \geq 0\end{aligned} \tag{23b}$$

where vectors $\boldsymbol{H}$ are generalised directions associated at contact points with local unit vectors $\boldsymbol{n}_j^{(i)}$ and $\boldsymbol{n}_j^{(i+1)}$. Inequalities (23a) and (23b) are in general different; they coincide only if the joint is closed. The consequence is that the contact laws imply different generalised directions $\boldsymbol{H}$ and reactions $\boldsymbol{\Phi}$. Relationship (23a) gives

Signorini's contact law:

$$R^{(i,i+1)}_{n_j^{(i)}}\left(\dot{r}^{(i+1)}_{Q,n_j^{(i)}}-\dot{r}^{(i)}_{P,n_j^{(i)}}\right)=\left(\boldsymbol{\Phi}^{(i+1)^T}_{Q,n_j^{(i)}}\dot{\boldsymbol{u}}^{(i+1)}-\boldsymbol{\Phi}^{(i)\ T}_{P,n_j^{(i)}}\dot{\boldsymbol{u}}^{(i)}\right)=0 \tag{24}$$

while Coulomb's law governing friction is:

$$R^{(i,i+1)}_{t_j^{(i)}}\left(\dot{r}^{(i+1)}_{Q,t_j^{(i)}}-\dot{r}^{(i)}_{P,t}\right)=\left(\boldsymbol{\Phi}^{(i+1)^T}_{Q,t_j^{(i)}}\dot{\boldsymbol{u}}^{(i+1)}-\boldsymbol{\Phi}^{(i)\ T}_{P,t_j^{(i)}}\dot{\boldsymbol{u}}^{(i)}\right)\leq 0 \tag{25}$$

Analogous, although different, expressions are obtained from (23b).

3.2 Dynamics Equations and Outlines of the Method Proposed

With reference to system (O, x, y) fixed on Γ consider the equation of motion for the arch, obtained from d'Alembert's principle:

$$\sum_{i=1}^{n}\left(-\ddot{\boldsymbol{u}}^{(i)}+\boldsymbol{S}^{(i)}+\boldsymbol{\Psi}_P^{(i+1,i)}+\boldsymbol{\Psi}_Q^{(i-1,i)}\right)^T\overline{\dot{\boldsymbol{u}}^{(i)}}=0 \tag{26}$$

where $\ddot{\boldsymbol{u}}^{(i)}$ is the acceleration, $\boldsymbol{S}^{(i)}$ the active force, $\overline{\dot{\boldsymbol{u}}^{(i)}}$ the admissible velocity, and $\boldsymbol{\Psi}_P^{(i+1,i)}$ and $\boldsymbol{\Psi}_Q^{(i-1,i)}$ the reactions transmitted to *i-th* voussoir by the contiguous ones.

Since Signorini's and Coulomb's laws do not reduce the degrees of freedom, it seems that the dynamics of *i-th* voussoir:

$$\left(-\ddot{\boldsymbol{u}}^{(i)}+\boldsymbol{S}^{(i)}+\boldsymbol{\Psi}_P^{(i+1,i)}+\boldsymbol{\Psi}_Q^{(i-1,i)}\right)^T\overline{\dot{\boldsymbol{u}}^{(i)}}=0\quad i=1,\ldots,n \tag{27}$$

cannot be solved, as for the single block, unless the whole arch dynamics is, since reactions transmitted by the two contiguous voussoirs depend on their dynamics. A classical procedure (Lötstedt 1982; Glocker and Pfeiffer 1992) would be that of adopting an augmented Lagrangian multipliers method, by using reactions as multipliers and Eqs. (23a)–(25) as constraints. In this case, the fulfilment of Signorini's and Coulomb's laws is equivalent to the Kuhn-Tucker condition corresponding to the optimal solution of a quadratic programming problem; an iterative procedure is thus necessary and the mathematical problem requires inversion of matrices of great dimension, equal to the number of degrees of freedom plus constraints. In the case of the arch, however, matrices have elements different from zero only at the sides of the principal diagonal, since only contiguous voussoirs interact with each other; furthermore, activated mechanisms involve a number of mega-voussoirs lower than that of all the voussoirs.

Moreover, since the dynamics evolves starting from given initial positions and velocities according to a given mechanism, the instantaneous rotation centres are given. This means that the starting of relative either rocking or sliding-rocking, as of relative sticking or sliding, corresponds—as for the single block—to the same contact centres; whether the mechanism changes in the following motion depends only on the values and directions of reactions, which determine possible new instantaneous rotation centres. This is the reason why limit analysis with finite friction seems undetermined, unless contact laws are verified.

Both persistency and variation of the activated mechanism thus depend on either the fulfilment of Signorini's and Coulomb's laws or reaching the limit of their admissible sets; both require the determination of contact reactions—the main unknowns of the problem.

It will be demonstrated that the indeterminacy of arch dynamics can be eliminated by appropriate considerations on the relationship between the centre of instantaneous rotation of a central mega-voussoir and allowed reactions transmitted to it. A hierarchical iterative procedure is thus required, concerning at each step a number of joints at most equal to that of activated mega-voussoirs. A first level of iteration concerns only the boundary joints of mega-voussoirs; while a second level—at which intermediate joints are checked—can restart the first level of iteration. Observe that any numerical algorithm of mathematical programming requires an iterative procedure, involving at each step a number of unknowns equal to the number of all the degrees of freedom plus constraints.

Once the indeterminacy at boundary joints of mega-voussoirs has been eliminated—albeit tentatively –, contact reactions at intermediate joints can be determined by propagating the dynamic balance in the respect of contact laws. Note that it is the reaching of Coulomb's cone limit that requires the use of the iterative procedure, while that of Signorini's corresponds to loss of contact and then to probable collapse of the arch.

The starting of sliding-rocking of a mega-voussoir with respect to the contiguous one can be detected; since the new mechanism starts with null relative velocity at contact points, sliding-rocking effects are obtained in the motion that follows as a consequence of the dynamics and reaction along Coulomb's cone. Only for open joints, since Signorini's and Coulomb's laws are both split into two, which contact point slides with respect to the joint of contiguous mega-voussoir can be foreseen. In this case, the reaction is along Coulomb's cone at one joint, and internal at the other one; otherwise, if both reactions are along Coulomb's cone, as for closed joints, which point slides is given only by dynamics.

With reference to intermediate joints, the starting of either relative sliding or sliding-rocking for reaching Coulomb's cone limit depends on the contact points position, internal to the joint or at its boundary, respectively; the last case occurs when one contact centre at the boundary of a mega-voussoir is split into two, the second lying at the nearest joint and at the same side (extrados or intrados). The imposed reactions both along Coulomb's cone at the considered intermediate joint—since it is initially closed—vary with respect to those of relative sticking and determine a variation also at successive joints until the boundary of the

mega-voussoir is reached. As a consequence, the reaction acting on the opposite boundary also varies, and both the first and second levels of iteration restart until convergence.

In contrast, when the contact centre bounding a mega-voussoir is split into two—the second lying on same side at the extrados or intrados—and Coulomb's law is respected the iterative procedure is not required.

The greatest number of steps of iteration are therefore required only when Coulomb's limit is reached for variation of both size and number of elements of a mega-voussoir, while any numerical algorithm of mathematical programming is characterised by a number of steps exponentially proportional to that of unknowns.

Finally, note that numerical platforms of the literature use the discrete elements method with great difficulties related to the elimination of high frequencies, while the present formulation is based on the rigidity assumption.

These among others are the reasons why an analytical approach is proposed by propagating dynamics balance from a mega-voussoir to its contiguous and all intermediate joints.

3.3 Starting Motion and Dynamic Balance: First Level Iteration

By referring to the results obtained for the single block, remember that both rocking and sliding-rocking mechanisms require contact centre at joint boundaries, while resting and sliding correspond to contact centre internal to the joint. Moreover, remember that it is friction, which decides the loss of tangential contact, so that we can assume tentatively that it is maintained unless contact laws impose the contrary.

Admissible velocities for the generic voussoir require that admissible mechanisms for the whole arch be identified. Moreover, in any rotational arch mechanism, if *i-th* voussoir rotates around intrados at $(j-1)$-*th* joint, its maximal interaction with $(i+1)$-*th* voussoir is at the extrados of *j-th* joint. Therefore, rotational mechanisms are characterized by alternate hinges at the extrados and intrados respectively, even if each of such hinges can be split into two for a dynamical thrust line going out from a single voussoir; while, if the arch is at rest and external excitation is increasing starting from zero, the most probable mechanism is characterised by the lowest number of alternate hinges at the extrados and intrados.

Consider the dynamics excited by increasing horizontal ground motion $\ddot{x}_{\mathrm{O}} = k_{\mathrm{s}}(t)g$ starting from zero, and determine the rotational starting mechanism; by disregarding reactions since contacts are governed by normality rules, the necessary condition for starting motion becomes:

$$\min_{k_s} \sum_{i=1}^{n} \boldsymbol{S}^{(i)\mathrm{T}} \overline{\dot{\boldsymbol{u}}^{(i)}} = 0 \tag{28}$$

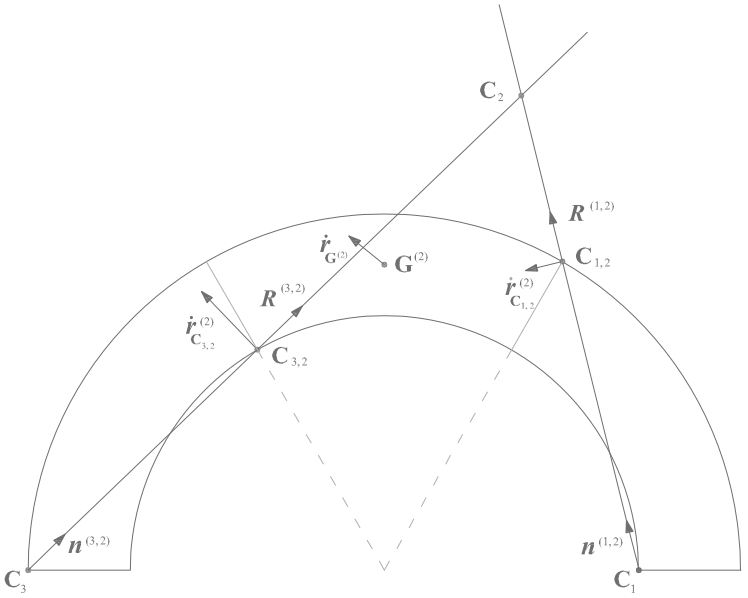

Fig. 10 Scheme of the starting rotational mechanism

By increasing the ground acceleration, null mechanisms $\dot{\boldsymbol{u}}^{(\mathrm{i})}$ are firstly admissible; they correspond to thrust lines with at most three alternate hinges at the extrados and intrados. In this case, the possibility of a mechanism with pure relative sliding at some intermediate joint, even improbable, could be examined; for arches subjected only to their own weight this is the mixed mechanism identified in (Sinopoli *et al.* 2007).

Once four alternate hinges are formed, the well-known mechanism for asymmetric loads usually determined by an upper approach appears. The arch can thus be considered as made of only three mega-voussoirs; label them by index k, with $k = 1,2,3$, and contact centres positions (Fig. 10) by C_1, $C_{1,2}$, $C_{2,3}$, and C_3. Contact centres define the instantaneous rotation centre C_2 of second mega-voussoir, lying at the intersection of straight lines crossing points C_1 and $C_{1,2}$, and C_3 and $C_{2,3}$, respectively; C_2 does not vary in the following motion only if tangential contacts at all voussoirs contact centres are maintained.

The identification of contact centres at intermediate joints inside each mega-voussoir and checking of Signorini's and Coulomb's conditions at each joint require that reactions acting on each mega-voussoir be determined. To this aim, since the main role is played by second mega-voussoir, consider its dynamics equation:

$$\ddot{\boldsymbol{u}}^{(2)} - \boldsymbol{S}^{(2)} = +\boldsymbol{\Psi}_{\mathrm{C}_{2,3}}^{(3,2)} + \boldsymbol{\Psi}_{\mathrm{C}_{1,2}}^{(1,2)} \tag{29}$$

If Coulomb's law is verified at $C_{1,2}$ and $C_{2,3}$, but also at C_1 and C_3, reactions $\boldsymbol{R}^{(1,2)}$ and $\boldsymbol{R}^{(3,2)}$ evaluated in the system $(\boldsymbol{t}_o, \boldsymbol{n}_o)$ are parallel to unit vector $\boldsymbol{n}^{(1,2)}$ and $\boldsymbol{n}^{(3,2)}$, in line with points $C_{1,2}$ and C_2, and $C_{2,3}$ and C_2, respectively; thus: $\boldsymbol{R}^{(1,2)} = -\boldsymbol{R}^{(2,1)} = R^{(1,2)}\boldsymbol{n}^{(1,2)}$ and, similarly: $\boldsymbol{R}^{(3,2)} = -\boldsymbol{R}^{(2,3)} = R^{(3,2)}\boldsymbol{n}^{(3,2)}$. In fact, since the dynamics of second mega-voussoir is modulated by reactions $\boldsymbol{R}^{(1,2)}$ and $\boldsymbol{R}^{(3,2)}$ crossing contact centres $C_{1,2}$ and $C_{2,3}$ and second mega-voussoir rotates around C_2, the resultant of $\boldsymbol{R}^{(1,2)}$ and $\boldsymbol{R}^{(3,2)}$ necessarily crosses the instantaneous rotation centre C_2.

Thus, since inequalities (23a) and (23b) give: $\dot{\boldsymbol{r}}^{(1)}_{C_{1,2}} = \dot{\boldsymbol{r}}^{(2)}_{C_{1,2}}$, reactions $\boldsymbol{R}^{(1,2)}$ and $\boldsymbol{R}^{(2,1)}$ are orthogonal to $\dot{\boldsymbol{r}}^{(2)}_{C_{1,2}}$ and $\dot{\boldsymbol{r}}^{(1)}_{C_{1,2}}$, respectively; and, similarly, $\boldsymbol{R}^{(3,2)}$ and $\boldsymbol{R}^{(2,3)}$ are orthogonal to $\dot{\boldsymbol{r}}^{(2)}_{C_{2,3}}$ and $\dot{\boldsymbol{r}}^{(3)}_{C_{2,3}}$. A normality rule therefore governs generalised reactions and velocities at relative contact centres:

$$\begin{aligned} \boldsymbol{\Psi}^{(1,2)\mathrm{T}}_{C_{1,2}}\dot{\boldsymbol{u}}^{(2)} &= \boldsymbol{\Psi}^{(2,1)\mathrm{T}}_{C_{1,2}}\dot{\boldsymbol{u}}^{(1)} = 0 \\ \boldsymbol{\Psi}^{(3,2)\mathrm{T}}_{C_{2,3}}\dot{\boldsymbol{u}}^{(2)} &= \boldsymbol{\Psi}^{(2,3)\mathrm{T}}_{C_{2,3}}\dot{\boldsymbol{u}}^{(3)} = 0 \end{aligned} \tag{30}$$

Moreover, since reactions $\boldsymbol{\Psi}^{(1,2)}_{C_{1,2}}$ and $\boldsymbol{\Psi}^{(3,2)}_{C_{2,3}}$ can be rewritten as:

$$\begin{aligned} \boldsymbol{\Psi}^{(1,2)}_{C_{1,2}} &= R^{(1,2)}\mathbf{N}^{(2)}_{C_{1,2}}\boldsymbol{n}^{(1,2)} = R^{(1,2)}\boldsymbol{H}^{(2)}_{C_{1,2}} \\ \boldsymbol{\Psi}^{(3,2)}_{C_{2,3}} &= R^{(3,2)}\mathbf{N}^{(2)}_{C_{2,3}}\boldsymbol{n}^{(3,2)} = R^{(3,2)}\boldsymbol{H}^{(2)}_{C_{2,3}} \end{aligned} \tag{31}$$

scalar values of reactions $R^{(1,2)}$ and $R^{(3,2)}$ become flux along the generalised directions $\boldsymbol{H}^{(2)}_{C_{1,2}}$ and $\boldsymbol{H}^{(2)}_{C_{2,3}}$ associated with $\boldsymbol{n}^{(1,2)}$ and $\boldsymbol{n}^{(3,2)}$, and similarly for $R^{(2,1)}$ and $R^{(2,3)}$. Equation (29) assumes therefore a form very useful for dynamic balance:

$$\ddot{\boldsymbol{u}}^{(2)} - \boldsymbol{S}^{(2)} = R^{(3,2)}\boldsymbol{H}^{(2)}_{C_{2,3}} + R^{(1,2)}\boldsymbol{H}^{(2)}_{C_{1,2}} \tag{32}$$

In fact, from (30) to (31) it follows that both $\boldsymbol{H}^{(2)}_{C_{1,2}}$ and $\boldsymbol{H}^{(2)}_{C_{2,3}}$, as $\boldsymbol{\Psi}^{(1,2)}_{C_{1,2}}$ and $\boldsymbol{\Psi}^{(3,2)}_{C_{2,3}}$, belong to the plane $\pi^{(2)}$ orthogonal to $\dot{\boldsymbol{u}}^{(2)}$. By projecting (32) on plane $\pi^{(2)}$:

$$\ddot{\boldsymbol{u}}^{(2)}_{\pi} - \boldsymbol{S}^{(2)}_{\pi} = R^{(3,2)}\boldsymbol{H}^{(2)}_{C_{2,3}} + R^{(1,2)}\boldsymbol{H}^{(2)}_{C_{1,2}} \tag{33}$$

since the centripetal acceleration $\ddot{\boldsymbol{u}}^{(2)}_{\pi} = -\dot{\boldsymbol{N}}^{(2)\mathrm{T}}_{C_2}\dot{\boldsymbol{u}}^{(2)}$ is a known quantity, the dynamic balance assumes a static character; values $R^{(1,2)}$ and $R^{(3,2)}$ of transmitted reactions, like their generalised expressions $\boldsymbol{\Psi}^{(1,2)}_{C_{1,2}}$ and $\boldsymbol{\Psi}^{(3,2)}_{C_{2,3}}$, can be evaluated.

Contact laws must now be verified at each of the two joints bounding second voussoir, by decomposing $\boldsymbol{\Psi}^{(1,2)}_{C_{1,2}}$ and $\boldsymbol{\Psi}^{(3,2)}_{C_{2,3}}$ along the corresponding generalised normal and tangential directions; having satisfied contact laws, which can also imply starting of sliding-rocking, reactions $\boldsymbol{\Psi}^{(1,2)}_{C_{1,2}}$ and $\boldsymbol{\Psi}^{(3,2)}_{C_{2,3}}$ are tentatively determined.

By a similar procedure through the dynamic balance of first and third mega-voussoirs, the opposites of $R^{(1,2)}$ and $R^{(3,2)}$ allow us to determine $\boldsymbol{\Psi}_{C_1}^{(0,1)}$ and $\boldsymbol{\Psi}_{C_3}^{(4,3)}$ and, if Coulomb's limit of admissible solutions is reached at either or both joints, both $\boldsymbol{\Psi}_{C_{1,2}}^{(1,2)}$ and $\boldsymbol{\Psi}_{C_{2,3}}^{(3,2)}$ vary and the iteration continues until convergence.

Having tentatively determined $\boldsymbol{\Psi}_{C_1}^{(0,1)}$ and $\boldsymbol{\Psi}_{C_3}^{(4,3)}$, and $\boldsymbol{\Psi}_{C_{1,2}}^{(1,2)}$ and $\boldsymbol{\Psi}_{C_{2,3}}^{(3,2)}$ at the first level, the evaluation of contact reactions and checking of contact laws can be extended at intermediate joints of second mega-voussoir, as to those of first and third mega-voussoirs.

3.4 Second Level of Iteration at Intermediate Contact Centres

The evaluation of reactions acting at intermediate joints is performed starting from either boundary of second mega-voussoir, and checking all the joints up to the other boundary. At the first joint nearest either boundary, $\boldsymbol{\Psi}_{C_{1,2}}^{(1,2)}$ or $\boldsymbol{\Psi}_{C_{2,3}}^{(3,2)}$ is treated as a known force, which determines an augmented $\boldsymbol{S}^{(i)*}$ and gives the reaction at the successive joint. In this case, however, candidate and antagonist contact centres are unknown; they are identified by checking the possibility of relative motion, as for a starting mechanism. As an example, with reference to *j-th* joint by starting from the $(j-1)$-*th* one, express the tangential position of the unknown centre $P^{(i)}$ as a linear combination of intrados $A^{(i)}$ and extrados $B^{(i)}$ positions:

$$r_{P,t}^{(i)} = (1-e)\, r_{A,t}^{(i)} + e\, r_{B,t}^{(i)} \qquad 0 \le e \le 1 \tag{34}$$

and determine the contact centre of the virtual mechanism of relative rotation $\overline{\dot{\boldsymbol{u}}_P^{(i,i+1)}}$ satisfying:

$$\overline{\dot{\boldsymbol{u}}_P^{(i,i+1)}}^{T} \boldsymbol{S}^{(i)*} = 0 \tag{35}$$

The value of e so obtained identifies the contact centre $P^{(i)}$ and the reaction $\boldsymbol{\Psi}_P^{(i,i+1)}$ transmitted at *j-th* joint by *i-th* to $(i+1)$-*th* voussoir. If point $P^{(i)}$ is internal to the joint and Coulomb's law is satisfied, the mechanism does not change in the motion which follows, and checking can continue at successive intermediate joints; alternatively, pure sliding can start and the reaction along Coulomb's cone determines the variation of contact reactions from that joint to successive ones, until the boundary of mega-voussoir is reached. As a consequence, the reaction at the opposite boundary varies, and both first and second levels of iteration restart until convergence. On the contrary, if point $P^{(i)}$ lies either at extrados or intrados of the joint nearest that bounding the mega-voussoir, at same side of its contact centre, the mechanism changes in the following motion with no need of iterative procedure unless sliding-rocking is activated.

Similarly, reactions transmitted at all intermediate joints of first and third mega-voussoirs can be evaluated and checked up to the springing, and if necessary the iterative procedure is restarted until convergence. Having determined contact reactions through the method proposed, the equation of motion for each mega-voussoir can finally be integrated.

3.5 Dynamic Evolution and Mechanism Variation

The analysis here proposed, although aimed at identifying the starting motion, also holds during dynamics evolution according to a given mechanism.

The dynamics evolves starting from given initial positions and velocities; thus, if the activated mechanism is known, adherence to Signorini's and Coulomb's laws can be checked at each contact centre and, if verified, allows the maintainance of the mechanism in the motion which follows.

On the contrary, if the reaction required at any contact centre reaches Coulomb's limit of admissible solutions, the mechanism changes in the following motion depending on the position of the contact centre.

If it is either at the extrados or intrados of contiguous mega-voussoirs, with open contact joints, the projection of the determined contact reactions along the two local unit vectors systems identifies which contact point slides with respect to the contiguous joint, only if the reaction is along Coulomb's cone at either joint, and internal at the other one; otherwise, if both reactions are along Coulomb's cone, as for a closed joint, which contact point slides is given by dynamics. If the contact centre belongs to an intermediate joint of a mega-voussoir, relative either sliding—if allowed—or sliding-rocking can start with consequent variation of the number of mega-voussoirs involved in the mechanism.

Finally, it is worthwhile to note that if at any time and at any joint Signorini's set reaches a zero gap, the local contact is lost with consequent probable collapse of the arch.

4 Conclusions

The paper extends previous research of the author (Sinopoli 1997) on the dynamic modelling of a rigid body simply supported on a moving boundary. Its main purpose is the dynamic modelling of the masonry arch, treated as a system of n voussoirs with frictional unilateral contacts at each joint and dynamics governed by Signorini's and Coulomb's laws. The difficulties of the dynamics formulation are:

(a) the choice of the reference system and Lagrangian coordinates to write the equations of motion for each voussoir and each mega-voussoir, obtained by assembling one or many voussoirs in the activated mechanism;

(b) the evaluation of the principal unknowns of the dynamics, namely, the contact reactions acting at the two boundary joints of each mega-voussoir—and then of each voussoir—on which accelerations and velocities of the following motion depend.

An analytical procedure is proposed to write the equations of motion and to identify, for each voussoir in accordance with Signorini's and Coulomb's laws, the contact reactions as a function of active forces and instantaneous velocities of contact points. First, the modelling is given for the single block, to guide the understanding on how Signorini's and Coulomb's laws can be checked at contact point by identifying both the value of the generalised reaction and the persistency or variation of the activated mechanism. The formalism is then extended to the arch; new theoretical questions related to the arch typology are discussed and solved. The method is based on the key idea of transforming the dynamical modelling into an equivalent problem of "static" balance, by using for each element projecting techniques in the configuration space.

The indeterminacy of the arch is eliminated through an iterative procedure by propagating the dynamic balance from a selected mega-voussoir to contiguous ones, and then to all the voussoirs. The iterative procedure is activated only if Coulomb's cone limit is reached at any joint; it concerns a number of joints at most equal to that of the activated mega-voussoirs. The iterative procedure is thus not limiting and not time consuming with respect to other methods; it does not alter the solution, since the tentative solution at the first step of iteration is that for relative sticking or rocking, and corresponds at any step to instantaneous values of active forces, positions and velocities.

Having determined the contact reactions at each joint, the equations of motion can be integrated by either an explicit or implicit numerical procedure; in particular, an implicit procedure does not require evaluation of the acceleration, since the velocity of the following motion is obtained by that of the previous one plus the integral of active forces and reactions.

In conclusion, the paper presents a consistent analytical formulation, indicating also the computational procedure to implement a numerical platform for the dynamic analysis of the masonry arch.

Appendix: List of Symbols

C_k, $C_{k,k+1}$	Absolute and relative instantaneous rotation centres in the arch mechanism
g	Gravity acceleration
G	Mass centre of the block
$G^{(i)}$	Mass centre of *i-th* voussoir
$\boldsymbol{H}^{(\mathrm{i})}_{\mathrm{P,n_j}^{(i)}}$	Generalised direction associated with unit vector $\boldsymbol{n}_{\mathrm{j}}^{(\mathrm{i})}$ at point $P^{(\mathrm{i})}$ of *i-th* mega-voussoir

$\boldsymbol{H}^{(k+1)}_{C_{k,k+1}}$	Generalised direction associated with $\boldsymbol{n}^{(k,k+1)}$ at point $C_{k,k+1}$ of $(k+1)$-*th* mega-voussoir
i, j	Counters of arch voussoirs and joints, respectively
I_n, I_t	Normal and tangential impulsive reactions
k	Counter of mega-voussoirs in the arch mechanism
$k_s(t)$	Acceleration of the ground motion in g units
$\boldsymbol{n}^{(k,k+1)}$	Unit vector lined with contact and rotation centres of *k-th* and $(k+1)$-*th* mega-voussoirs
$\mathbf{N}_P$	Gradient operator of the position of point P
$\boldsymbol{N}_{P,n}, \boldsymbol{N}_{P,t}$	Normal and tangential vectors of the gradient operator $\mathbf{N}_P$
$\dot{\boldsymbol{N}}_{P,n}, \dot{\boldsymbol{N}}_{P,t}$	Normal and tangential vectors of derivative of $\mathbf{N}_P$
$\boldsymbol{N}_A{}^-, \boldsymbol{N}_A{}^+$	Negative and positive generalised Coulomb's boundaries for contact at point A
$\mathbf{N}^{(i)}_P$	Gradient operator of the position of point $P^{(i)}$ belonging to *i-th* voussoir of the arch
$\boldsymbol{N}^{(i)}_{P,n}, \boldsymbol{N}^{(i)}_{P,t}$	Normal and tangential vectors of gradient operator $\mathbf{N}^{(i)}_P$ of *i-th* voussoir
(O, x, y)	Reference system fixed on boundary Γ
P	Generic point of the block
Q	Centre of contact for the block
$P^{(i)}_j, Q^{(i+1)}_j$	Antagonist and candidate contact points at *j-th* joint of the arch
$r_{P,t}$	Tangential position of point P
$\dot{\boldsymbol{r}}_P$	Velocity of point P
$\dot{r}_{P,n}, \dot{r}_{P,t}$	Normal and tangential velocities of point P
$\ddot{r}_{P,n}, \ddot{r}_{P,t}$	Normal and tangential accelerations of point P
$\dot{r}^+_{Q,n}, \dot{r}^+_{Q,t}$	Post-impact normal and tangential velocities of point Q
$\dot{\boldsymbol{r}}^{(i)}_P, \dot{\boldsymbol{r}}^{(i)}_Q$	Velocity of points $P^{(i)}$ and $Q^{(i)}$ belonging to *i-th* voussoir of the arch
$\dot{r}^{(i)}_{P,n^{(i)}_j}, \dot{r}^{(i+1)}_{Q,n^{(i)}_j}$	Normal velocity of antagonist $P^{(i)}$ and candidate $Q^{(i+1)}$ points in the system $(\boldsymbol{t}^{(i)}_j, \boldsymbol{n}^{(i)}_j)$
R_n, R_t	Normal and tangential reactions at contact point
$\boldsymbol{R}^{(i,i+1)}$	Reaction transmitted by *i-th* to $(i+1)$-*th* voussoir in $(\boldsymbol{t}_o, \boldsymbol{n}_o)$
$R^{(i,i+1)}_n, R^{(i,i+1)}_t$	Normal and tangential reactions transmitted by *i-th* to $(i+1)$-*th* voussoir in $(\boldsymbol{t}_o, \boldsymbol{n}_o)$
$R^{(i,i+1)}_{n^{(i)}_j}, R^{(i,i+1)}_{t^{(i)}_j}$	Normal and tangential reactions transmitted by *i-th* to $(i+1)$-*th* voussoir in $(\boldsymbol{t}^{(i)}_j, \boldsymbol{n}^{(i)}_j)$
$\boldsymbol{S}$	Generalised force active on the block
$\boldsymbol{S}^{\pi}$	Generalised active force in plane π
$\boldsymbol{S}^{(i)}$	Generalised force active on the *i-th* voussoir
t	Time instant
$(\boldsymbol{t}, \boldsymbol{n}), (\boldsymbol{t}_o, \boldsymbol{n}_o)$	Unit vectors associated with system (O, x, y) for the block and arch, respectively

$(\boldsymbol{t}_{\mathrm{j}}^{(\mathrm{i})}, \boldsymbol{n}_{\mathrm{j}}^{(\mathrm{i})})$	Local unit vectors system associated with *i-th* voussoir at *j-th* joint
$\overline{\dot{\boldsymbol{u}}}$	Generalised admissible velocity of the block
$\dot{\boldsymbol{u}}, \ddot{\boldsymbol{u}}$	Generalised velocity and acceleration of the block
$\overline{\dot{\boldsymbol{u}}^{+}}$	Generalised admissible post-impact velocity
$\dot{\boldsymbol{u}}^{-}, \dot{\boldsymbol{u}}^{+}$	Generalised pre-impact and post-impact velocities
$\dot{\boldsymbol{u}}_{\mathrm{A}}$	Mechanism with contact at point A
$\ddot{\boldsymbol{u}}_{\mathrm{A}}$	Generalised acceleration with contact at point A
$\ddot{\boldsymbol{u}}_{\mathrm{A,n}}, \ddot{\boldsymbol{u}}_{\mathrm{A,t}}$	Normal and tangential generalised accelerations in plane π for contact at point A
$\overline{\dot{\boldsymbol{u}}^{(\mathrm{i})}}$	Generalised admissible velocity of *i-th* voussoir
$\dot{\boldsymbol{u}}^{(\mathrm{i})}, \ddot{\boldsymbol{u}}^{(\mathrm{i})}$	Generalised velocity and acceleration of *i-th* voussoir
$\ddot{x}_{\mathrm{O}}$	Acceleration of ground motion
$\Delta\dot{\boldsymbol{u}}$	Generalised velocity variation
Γ	Boundary of the rigid ground
μ	Friction coefficient
π	Plane to which $\boldsymbol{N}_{\mathrm{A,n}}$ and $\boldsymbol{N}_{\mathrm{A,t}}$ belong for $\dot{r}_{\mathrm{A,t}}$ equal to zero
π *	Plane to which $\boldsymbol{N}_{\mathrm{A,n}}$ and $\boldsymbol{N}_{\mathrm{A,t}}$ belong for $\dot{r}_{\mathrm{A,t}}$ different from zero
$\pi^{(2)}$	Plane orthogonal to mechanism $\dot{u}^{(2)}$ of the second mega-voussoir
$\boldsymbol{\Psi}_{\mathrm{C}_{1,2}}^{(1,2)}$	Generalised reaction transmitted by first to second mega-voussoir at $C_{1,2}$
$\boldsymbol{\Phi}_{\mathrm{P,n}_{\mathrm{j}}^{(\mathrm{i})}}^{(\mathrm{i})}, \boldsymbol{\Phi}_{\mathrm{P,t}_{\mathrm{j}}^{(\mathrm{i})}}^{(\mathrm{i})}$	Local generalised normal and tangential reactions at point $P^{(\mathrm{i})}$ of *i-th* voussoir
$\boldsymbol{\Psi}_{\mathrm{P}}^{(\mathrm{i,i+1})}$	Generalised reaction transmitted at point $P^{(\mathrm{i})}$ by *i-th* to $(i+1)$-*th* voussoir
$\boldsymbol{\Psi}_{\mathrm{Q,n}}, \boldsymbol{\Psi}_{\mathrm{Q,t}}$	Generalised normal and tangential reactions at point Q
$\boldsymbol{\Psi}_{\mathrm{Q,t}}^{*}$	Generic generalised reaction belonging to Coulomb's cone
$\boldsymbol{\Xi}_{\mathrm{Q,n}}, \boldsymbol{\Xi}_{\mathrm{Q,t}}$	Generalised normal and tangential impulses

References

Ageno, A., & Sinopoli, A. (2005). Lyapunov's exponents for non-smooth dynamics with impacts: Stability analysis of the rocking block. *International Journal of Bifurcation and Chaos, 15*(6), 2015–2039.

Ageno, A., & Sinopoli, A. (2010). Symmetry properties in the symmetry-breaking of non-smooth dynamical systems. *Journal of Computational and Nonlinear Dynamics, 5*(10), 1–9.

Augusti, G., & Sinopoli, A. (1992). Modelling the dynamics of large block structures. *Meccanica, 27*(3), 195–211.

Baggio, C., & Trovalusci, P. (2000). Collapse behaviour of three-dimensional brick-block systems using non-linear programming. *Structural Engineering and Mechanics, 10*(2), 181–195.

Clemente, P. (1998). Introduction to dynamics of stone arches. *Earthquake Engineering and Structural Dynamics, 27*(5), 513–522.

Cundall, P. A., & Strack, O. D. L. (1979). A discrete numerical model for granular assemblies. *Geotechnique, 29*(1), 47–65.

De Lorenzis, L., DeJong, M., & Ochsendorf, J. (2007). Failure of masonry arches under impulse base motion. *Earthquake Engineering and Structural Dynamics, 36*(14), 2119–2136.

Gilbert, M., & Melbourne, C. (1994). Rigid block analysis of masonry structures. *The Structural Engineer, 72*(21), 356–361.

Glocker, C., & Pfeiffer, F. (1992). Dynamical systems with unilateral contacts. *Nonlinear Dynamics, 3*(4), 245–259.

Heyman, J. (1969). The safety of masonry arches. *International Journal of Mechanical Sciences, 11*(4), 363–385.

Hogan, S. J. (1990). The many steady state responses of rigid block under harmonic forcing. *Earthquake Engineering and Structural Dynamics, 19*(7), 1057–1071.

Housner, G. W. (1963). The behavior of inverted pendulum structures during earthquakes. *Bulletin of Seismological Society of America, 53*, 403–417.

Jean, M. (1999). The non-smooth contact dynamics method. *Computer Methods in Applied Mechanics and Engineering, 177*(3–4), 235–257.

Livesley, R. K. (1978). Limit analysis of structures formed from rigid blocks. *International Journal for Numerical Methods in Engineering, 12*(12), 1853–1871.

Lötstedt, P. (1982). Mechanical systems of rigid bodies subject to unilateral constraints. *SIAM Journal on Applied Mathematics, 42*(2), 281–296.

Moreau, J. J. (1988). Unilateral contact and dry friction in finite freedom dynamics. In J. J. Moreau & P. D. Panagiotopoulos (Eds.), *Non-Smooth Mechanics and Applications, CISM Courses and Lectures* (Vol. 302, pp. 1–82). Wien: Springer.

Moreau, J. J. (1999). Numerical aspects of the sweeping. *Computer Methods in Applied Mechanics and Engineering, 177*(3–4), 329–349.

Moreau, J. J. (2005). An introduction to unilateral dynamics. In M. Frémond & M. Maceri (Eds.), *Novel Approaches in Civil Engineering, Notes in Applied and Computational Mechanics* (Vol. 14, pp. 1–46). Berlin: Springer.

Oppenheim, I. J. (1992). The masonry arch as a four-link mechanism under base motion. *Earthquake Engineering and Structural Dynamics, 21*(11), 1005–1017.

Orduna, A., & Lourenço, P. B. (2005). Three-dimensional limit analysis of rigid blocks assemblages. Part II: Load-path following solution procedure and validation. *International Journal of Solid and Structures, 42*(18–19), 5161–5180.

Rafiee, A., Vinches, M., & Bohatier, C. (2008). Application of the NSCD method to analyse the dynamic behaviour of stone arched structure. *International Journal of Solid and Structures, 45*(25–26), 6269–6283.

Sinopoli, A. (1987). Dynamics and impact in a system with unilateral constraints. The relevance of dry friction. *Meccanica, 22*(3), 210–215.

Sinopoli, A. (1997). Unilaterality and dry friction. A geometric formulation for two-dimensional rigid body dynamics. *Nonlinear Dynamics, 12*(4), 343–366.

Sinopoli, A. (2010). A semi-analytical approach for the dynamics of the stone arch. *Proceedings of ICE, Engineering and Computational Mechanics, 163EM3*, 167–178.

Sinopoli, A., Aita, D., & Foce, F. (2007). Further remarks on the collapse of masonry arches with Coulomb friction. In P. Lourenço, D. V. Oliveira, & A. Portela (Eds.), *Arch'07* (pp. 649–658). Multicomp: Guimarães.

Sinopoli, A., Corradi, M., & Foce, F. (1997). A modern formulation for pre-elastic theories on masonry arches. *Journal of Engineering Mechanics, 123*(3), 204–213.

Spanos, P. D., & Koh, A.-S. (1984). Rocking of rigid blocks due to harmonic shaking. *Journal of Engineering Mechanics, 110*(11), 1627–1643.